



TECHNICAL REPORT 2048  
September 2014

## Output from Linear Generator for VIV-driven Buoys

Wayne Liu  
Jack Dea  
Kyle Wendler  
Brian Dick  
**SSC Pacific**

Brian D'Angelo  
**American Society of  
Engineering Education (ASEE)**

Approved for public release.

SSC Pacific  
San Diego, CA 92152-5001



TECHNICAL REPORT 2048  
September 2014

## Output from Linear Generator for VIV-driven Buoys

Wayne Liu  
Jack Dea  
Kyle Wendler  
Brian Dick  
**SSC Pacific**

Brian D'Angelo  
**American Society of  
Engineering Education (ASEE)**

Approved for public release.

SSC Pacific  
San Diego, CA 92152-5001



**SSC Pacific**  
**San Diego, California 92152-5001**

---

---

**J. J. Beel, CAPT, USN**  
**Commanding Officer**

**C. A. Keeney**  
**Executive Director**

**ADMINISTRATIVE INFORMATION**

The Office of Naval Research administered and funded this In-house Laboratory Independent Research (ILIR) project. The Radiation Technologies Branch (Code 56480) of the Maritime Systems Division (Code 56400), SPAWAR Systems Center Pacific (SSC Pacific), San Diego, CA, performed the work described in this report. A member of the American Society for Engineering Education (ASEE) also worked on the project.

Released by  
J. E. Spencer, Head  
Composeable Service Services Branch

Under authority of  
C. Rainey, Head  
CMD and Control Tech &  
Experiment Division

**ACKNOWLEDGMENTS**

The authors are grateful for the SSC Pacific Internal R&D support provided by Dr. Dave Rees and the Office of Naval Research In-Laboratory Independent Research program. This research would not have been possible without the superb support and insight provided by Charles Coughran, Dave Aglietti, and John Lyons of the Scripps Institute of Oceanography Hydraulics Lab (La Jolla, CA).

This is a work of the United States Government and therefore is not copyrighted. This work may be copied and disseminated without restriction.

The citation of trade names and names of manufacturers in this report is not to be construed as official government endorsement or approval of commercial products or services referenced in this report.

Chatillon<sup>®</sup> is a registered trademark of AMETEK Inc.

## **EXECUTIVE SUMMARY**

### **OBJECTIVE**

Vortex Induced Vibration (VIV) methods were studied by Space and Naval Warfare Systems Center Pacific (SSC Pacific) as one approach for harvesting energy on deeply submerged platforms where slow current flow (0.5 knot), changing flow directions and ease of deployment and maintenance must often be considered. VIV motions of a cylindrical tube or buoy could typically achieve +/- one diameter oscillation displacements that can be used to drive or pump a power generation device.

FY13 work evaluated (1) the feasibility of 1-W power output from a linear magnetic generator that could fit inside a 10- to 12-inch (0.25- to 0.30-meter)-diameter buoy undergoing VIV oscillations in 0.5 knots (0.25 meter/second) flow, and (2) predictions of buoy VIV frequencies when carrying an internal pendulum for actuating a magnetic generator.

### **METHOD**

This project evaluated power generation from actuating a pair of 2-inch spherical neodymium magnets within a PVC pipe surrounded by multiple coil structures. Predictions of buoy oscillation frequencies that could drive magnet vs. coil structures were then developed using VIV, inverted pendulum, and mass-spring oscillation fundamentals.

### **SUMMARY AND RECOMMENDATIONS**

This report presents a linear generator system that could be used internally in an upright buoy to produce power. Simple power tests were conducted using machine and manual actuation of a pair of magnets within a copper coil-fitted tube and demonstrated 1.38- to 1.92-W outputs at linear actuation speeds of 11 inches per second.

A derivation of a non-dimensionalized math model was then presented for predicting oscillation frequencies of a submerged tethered buoy that could be used to actuate a linear generator. The model included a prediction of the buoy excitation frequencies due to vortex shedding. To match this excitation frequency with buoy natural frequencies, this model included coupling effects of an internal pendulum and added mass of the buoy, but excluded viscous damping. This model did not include coupling of the buoy motion on the vortex shedding frequencies.



## CONTENTS

<b>1. INTRODUCTION .....</b>	<b>1</b>
<b>2. LINEAR GENERATOR.....</b>	<b>3</b>
<b>3. MODELING VIV OSCILLATIONS .....</b>	<b>7</b>
3.1 MODELING BUOY EXCITATION AND NATURAL FREQUENCIES .....	7
3.2 BUOY WITH INTERNAL PENDULUM LOAD .....	9
<b>4. CONCLUSIONS .....</b>	<b>13</b>
<b>5. REFERENCES .....</b>	<b>15</b>

## Figures

1. FY13 work seeks to evaluate feasibility of 1W power output from linear generator that fits inside a 10- to 12-inch-diameter buoy and can be driven by vortex-induced vibrations (VIV) in 0.5-knot flow .....	1
2. Test setup for evaluating linear generator consisting of spherical magnet pair driven in/out of PVC pipe fitted with wraparound coils. Input force was controlled and measured by benchtop actuation device; voltage output of coils (open circuit and loaded) recorded by a spectrum analyzer device .....	3
3. Force applied at short end of lever arm over several cycles to actuate magnet plunger with various loading conditions. Actual force in driving magnet plunger is 4.9X less due to lever arm used to amplify displacement (see Figure 2) .....	4
4. Testing of linear generator showed that roughly 1 to 2 watts is possible when a pair of magnet spheres (2-inch-diameter) is hand-driven up/down through a five-coil array at a rate of ~ 11 inches/second. Power is increased when a magnet pair is brought closer together from 4 to 2.125 inches, creating a more compressed flux gradient and thus greater power generation when passing a coil.....	5
5. To optimize buoy oscillations for actuating an internal pendulum drive, various structural frequencies must be matched against vortex shedding frequencies by adjusting buoy and pendulum mass. Modeling methods will be presented that can be used to align such frequencies.....	7
6. Free-body diagrams of (left) heavy or negatively buoyant pendulum and (right) light or positively buoyant pendulum.....	9
7. Spring-mass diagram for buoy mass $M_b$ and internal pendulum mass $M_p$ undergoing VIV-driven excitation .....	9
8. Natural frequency for range of $m^*$ ( $m_b$ /mass of displaced fluid) and $p^*$ (pendulum mass/buoy mass) ratios are modeled. Excitation frequency $f_{vs}$ is fixed (horizontal line) for given buoy diameter and flow velocity; $f_{vs}$ matches natural buoy frequencies at line intersections.....	11

## Table

1. Diameter, resistance, and turns of wraparound coils on PVC pipe.....	3
---	---



# 1. INTRODUCTION

Within the offshore structural and civil engineering communities, vortex induced vibrations (VIV) are often responsible for annoying acoustical tones, or in extreme cases, outright structural failures. Thus, much work has focused over the past few decades in designing structures to minimize or defeat VIV. However, one area in which VIV is most welcome is in the field of energy harvesting. In this application, VIV can be exploited and even amplified to oscillate magnetic fields against coils to generate voltage and thus power.

Large-scale demonstration of VIV-based energy harvesting was accomplished by Bernitsas of Vortex Hydro Energy and their Vortex Induced Vibration Aquatic Clean Energy (VIVACE) platform, which was installed in the St. Clair River in Port Huron, MI [1]. This particular platform used river flow to drive an array of large diameter, vertically oscillating cylinders and sought to prove the viability of tapping low-speed water flows for commercial power. Small-scale commercial demonstration of vortex or flow induced vibrations in air was performed by Frayne [2] using the Wind Belt, which would oscillate end-mounted magnets in and out of coils.

While previous designs show that significant power can be harvested from VIV, there are still many design considerations that have yet to be answered. For instance, how could VIV be exploited for generating power in deeply submerged ocean applications where slow current flow (0.5 knot), changing flow directions and ease of deployment and maintenance are critical drivers of any design? To address this problem, SPAWAR Systems Center Pacific (SSC Pacific) has conducted research using small (0.5-inch-diameter) and large-scale (10-inch-diameter) cylinders to produce VIV for power generation.

FY13 work (see Figure 1) evaluated the feasibility of 1W power output from a linear magnetic generator that can fit inside a 10- to 12-inch (0.25- to 0.30-meter)-diameter buoy and be driven by VIV in 0.5 knots (0.25 meters/second) flow. Additional work at SSC Pacific will design a pendulum drive within a buoy to actuate the linear generator.

This paper will discuss: (1) power output that can be expected when cycling a pair of 2-inch spherical neodymium magnets within a PVC pipe fitted with multiple coil structures, and (2) predictions of buoy oscillation frequencies that can be used to actuate an internal pendulum device for driving magnet/coil structures.

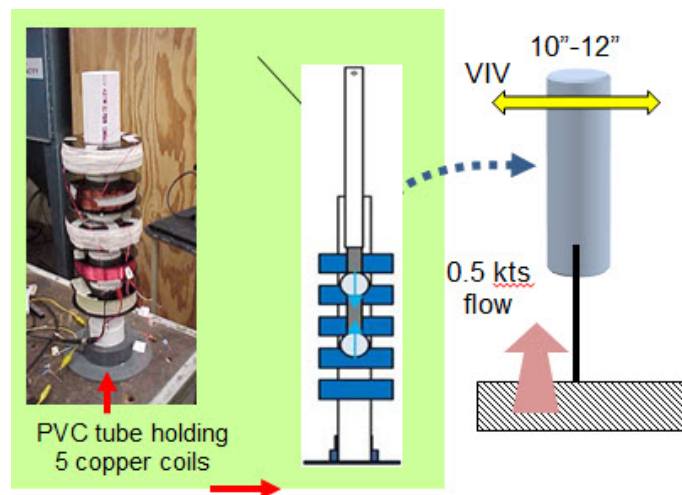


Figure 1. FY13 work seeks to evaluate feasibility of 1W power output from linear generator that fits inside a 10- to 12-inch-diameter buoy and can be driven by vortex-induced vibrations (VIV) in 0.5-knot flow.



## 2. LINEAR GENERATOR

To characterize a linear generator arrangement that could likely be integrated within and driven by VIV oscillations of an upright tethered buoy, researchers constructed a test setup to measure magnet travel, actuation force, and resultant voltage outputs across a series of copper coils. Figure 2 shows a photo and the dimensions of the setup, including force input and measurement device (Chatillon® TCD225 Force Measurement system), lever arm for amplifying displacement input, magnet plunger, and PVC pipe with copper coils.

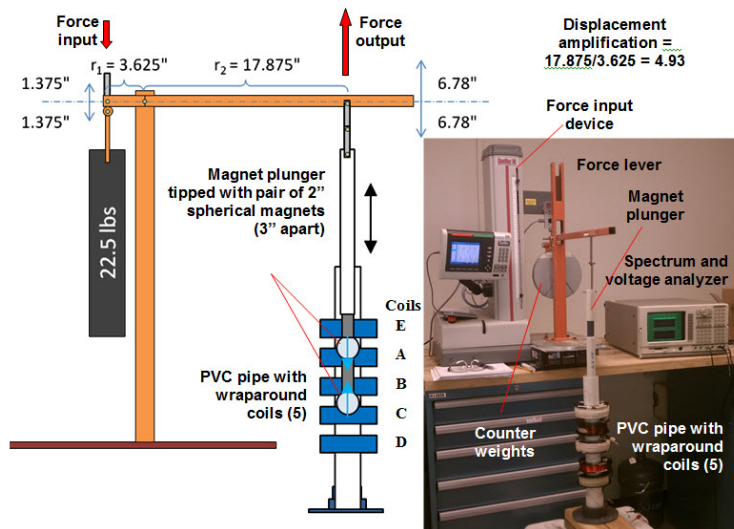


Figure 2. Test setup for evaluating linear generator consisting of spherical magnet pair driven in/out of PVC pipe fitted with wraparound coils. Input force was controlled and measured by benchtop actuation device; voltage output of coils (open circuit and loaded) recorded by a spectrum analyzer device.

Since the total actuation distance of the force input device was limited to 2.75 inches, a lever arm amplified the stroke input by 4.93X to raise the magnet plunger  $\pm 6.78$  inches above and below the horizontal axis (total 13.56-inch stroke distance). The magnet plunger served to drive two 2-inch-diameter neodymium magnet spheres (separated by a 3-inch spacer) in/out of a 2.0-inch ID PVC pipe, upon which five copper coils were affixed.

Figure 3 shows force input over time/distance for driving the pair of magnet spheres up and down: (1) without any constraining PVC pipe structure--no tube, (2) inside the PVC pipe and with the coils unloaded—open circuit, and (3) inside the PVC pipe with resistor loads across the coils--loaded.

Table 1 lists the characteristics of the five coils wrapped around the PVC pipe.

Table 1. Diameter, resistance, and turns of wraparound coils on PVC pipe.

Coil	Diameter (inches)	Resistance (ohms)	Turns
E	5	33	1560
A	4.5	55	1560
B	5	33	1560
C	4.25	220	2600
D	4.5	55	1560

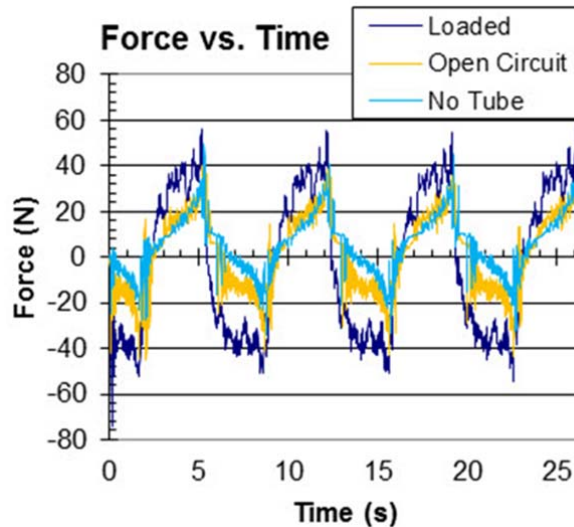


Figure 3. Force applied at short end of lever arm over several cycles to actuate magnet plunger with various loading conditions. Actual force in driving magnet plunger is 4.9X less due to lever arm used to amplify displacement (see Figure 2).

With matched resistor loads attached to the coils, a maximum force of 50 to 55 newton was delivered by the machine at the short end of the lever arm to actuate the magnet plunger; this translated to a maximum lifting force of 10 to 11 newton (4.9X less) imposed directly over the magnet plunger. The resultant power output (RMS) was measured as 0.148 watts by summing the outputs ( $V^2/R$ ) of the five resistors during a complete displacement cycle for the magnet plunger. A plunger displacement cycle consisted of two 13.6-inch strokes (down/up) covered in 6.6 seconds (~ 4 inches/second).

To evaluate power output when actuating the magnet plunger at a faster rate than the machine's maximum output of 27.2 inches (13.6 inches/stroke x 2 strokes) per 6.6 seconds, the plunger was disconnected from the lever arm and manually driven down and backed up within the PVC pipe in 2.5 seconds (~ 11 inches/second). Granted, this hand-driven magnet actuation is not precise, but serves only to provide a rough measure of what power is available when magnet actuation speed is increased.

Figure 4 shows the resultant power output when the pair of magnet spheres was hand driven while separated by 4.0-, 3.0-, and 2.125-inch steel spacers. Figure 4 shows that 1.38 to 1.92 watts was achieved when plunging a single pair of 2-inch-diameter spherical magnets past a five-coil array at speeds of roughly 11 inches per second.

When magnet pair separation is reduced from 4 to 2.125 inches, greater power is captured across the five coils (from 1.38 to 1.92 watts). This is likely due to the compression of the flux gradient between the two magnets, resulting in greater power. Flux compression is used in SSC Pacific-developed kinetic energy harvesters (KEHs) to increase power output [3].

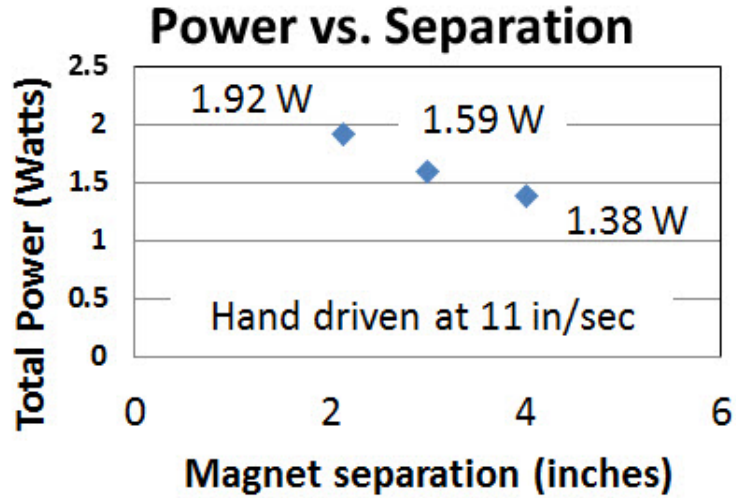


Figure 4. Testing of linear generator showed that roughly 1 to 2 watts is possible when a pair of magnet spheres (2-inch-diameter) is hand-driven up/down through a five-coil array at a rate of ~ 11 inches/second. Power is increased when a magnet pair is brought closer together from 4 to 2.125 inches, creating a more compressed flux gradient and thus greater power generation when passing a coil.



### 3. MODELING VIV OSCILLATIONS

The linear generator testing demonstrated the range of power output achievable for a buoy-compatible magnet/coil structure and magnet actuation force and speed inputs. Using this force and speed data as a design goal, we can begin to model a submerged tethered buoy to yield VIV oscillations for driving an internal pendulum actuator.

#### 3.1 MODELING BUOY EXCITATION AND NATURAL FREQUENCIES

Oscillation of a tethered submerged buoy can be optimized by synchronizing or matching its vortex shedding or flow excitation frequency ( $f_{vs}$ ) to its natural or resonant frequency ( $f_b$ ). However, the presence of a significant pendulum load inside the buoy will couple into the overall buoy oscillation and shift buoy resonant frequency ( $f_{bp}$ ) according to buoy mass ( $m_b$ ), pendulum spring constant ( $k$ ), and pendulum mass ( $m_p$ ). Figure 5 illustrates the myriad of variables at play that will produce the various oscillation frequencies that must be aligned to optimize buoy motion.

The frequency of flow excitation (vortex shedding,  $f_{vs}$ ) on submerged bodies can be determined by the well-known Strouhal number ( $St$ ), which relates  $f_{vs}$ , the cylinder diameter ( $D$ ), and cross flow velocity ( $U$ ) to a Reynolds number ( $Re$ ) dependent coefficient [4, 5]. For a cylinder in a wide range of flow conditions leading to an  $Re$  of 300 to  $10^5$ , Equation (1) shows that  $St$  can be approximated as 0.20 [5].

$$St = \frac{f_{vs}D}{U} = 0.20 \quad (1)$$

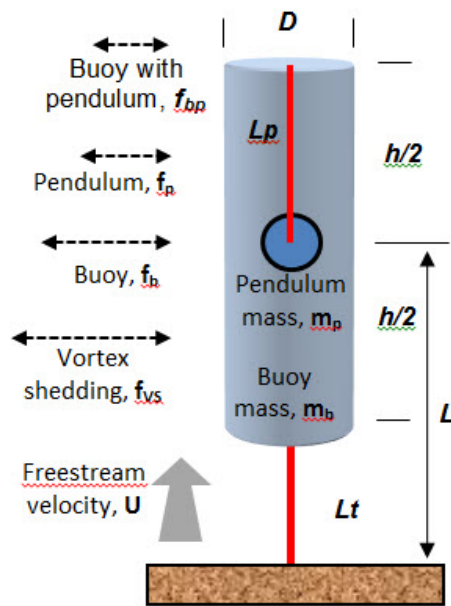


Figure 5. To optimize buoy oscillations for actuating an internal pendulum drive, various structural frequencies must be matched against vortex shedding frequencies by adjusting buoy and pendulum mass. Modeling methods will be presented that can be used to align such frequencies.

For flows in the scope of this research, where nominal  $D = 0.25$  meters and water velocity  $U = 0.25$  meters/second,  $Re = 62,500$ , and the flow excitation frequency  $f_{vs}$  is estimated by Strouhal number as 0.20 hertz or one oscillation cycle per 5 seconds. To optimize buoy oscillations for power generation, buoy and pendulum natural frequencies should be designed to match  $f_{vs}$ .

The natural frequency of a pendulum can easily be determined by Equation (2). This equation shows the angular frequency  $\omega$  as a function of the spring constant  $k$  and the total mass  $M$ . The spring constant of a tethered buoy is given by Equation (3). In this equation,  $m_b$  is the mass of the buoy,  $g$  is the gravity constant, and  $L$  is the length of the buoy tether when extended to the center of gravity. It is important to differentiate between total mass and buoy mass. Since this buoy will be completely submerged, it is important to account for the added mass of the buoy ( $m_a$ ). Therefore, the total mass  $M$  is a combination of the added mass ( $m_a$ ) and the buoy mass ( $m_b$ ) shown in Equation (4) [6].

$$\omega = \sqrt{\frac{k}{M}} \quad (2)$$

$$k = \frac{m_b g}{L} \text{ (hanging pendulum)} \quad (3)$$

$$M = m_b + m_a \quad (4)$$

The added mass  $m_a$  is easily calculated by Equation (5), provided by Berteaux [7]. Note that every shape has an individual equation for added mass and Equation 5 describes the added mass of a cylinder.

$$m_a = \rho_w V C_a. \quad (5)$$

In Equation (5),  $\rho_w$  is the fluid density,  $V$  is the volume of the cylinder, and  $C_a$  is the added mass coefficient (typically 1 for a cylinder).

In Equation (3), note that this is the spring constant of a hanging pendulum. The buoy, however, will essentially be an inverted pendulum. Comparison of the free-body diagrams in Figure 6 show how the spring constant should be adjusted to account for an inverted pendulum with a positively buoyant mass.

Using the methodology presented by Colwell (see Figure 6), the spring constant for a submerged, inverted pendulum is shown in Equation (6). Simply put, this equation states that the spring constant of an inverted pendulum is the difference between the buoyant and gravitational forces divided by the pendulum length (measured to center of mass).

$$k = \frac{(\rho_w V - m_b)g}{L} \quad (6)$$

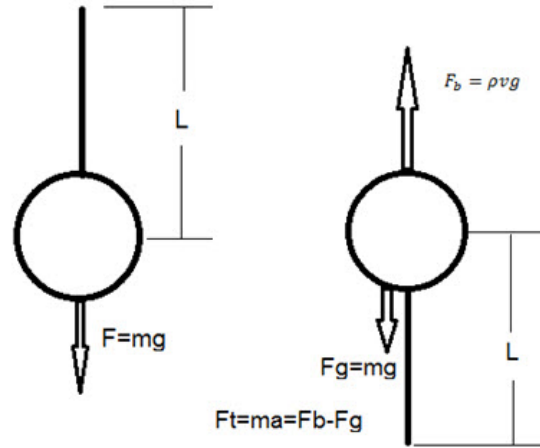


Figure 6. Free-body diagrams of (left) heavy or negatively buoyant pendulum and (right) light or positively buoyant pendulum.

Plugging Equations 4, 5, and 6 into Equation 2 will provide the natural frequency of a submerged buoy assuming no damping and no internal spring. This is shown in Equation (7).

$$\omega_b = \sqrt{\frac{(\rho_w V - m_b)g}{(m_b + \rho_w V C_a)L}} \quad (7)$$

Recognizing that  $m_b$  will always be a fraction of  $\rho_w V$  for a positively buoyant object, we can make use of a mass ratio  $m^*$  that is often used by VIV researchers [8, 9] to relate the mass of oscillating parts to the mass of the fluid displaced by the oscillating parts. A mass ratio less than 1 indicates a positively buoyant VIV platform, whereas  $m^* = 3$  indicates the oscillating parts are 3X heavier than their displaced fluids.

Essentially,  $m^* = m_b/m_{fd}$ . Then replacing  $m_b$  with  $\rho_w V m^*$ , Equation (7) can be reduced to

$$\omega_b = \sqrt{\frac{(1 - m^*)g}{(m^* + C_a)L}} \quad (8)$$

Equation (8) shows that buoy natural frequency  $\omega_b$  is a function of  $m^*$  (ratio of buoy mass to displaced fluid mass), the gravity constant, and length of tether to the center of buoy mass and is independent of buoy diameter  $D$ .

### 3.2 BUOY WITH INTERNAL PENDULUM LOAD

While Equation (8) describes the natural frequency of a submerged buoy, the design presented in this report seeks to utilize an internal pendulum to drive a linear generator and thus introduces a secondary internal spring-mass system. Figure 7 shows the entire system as a system of springs and masses connected in series.

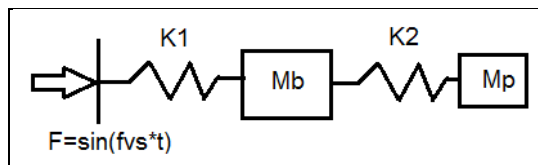


Figure 7. Spring-mass diagram for buoy mass  $M_b$  and internal pendulum mass  $M_p$  undergoing VIV-driven excitation.

Figure 7 shows a forcing frequency acting on two spring-mass systems in series. As conventional physics describes, there will be a coupling effect due to the second spring-mass system acting on the first spring-mass system and vice versa. Note that for now, all damping forces have been neglected. In 2008, Electro-Standards Laboratory and the University of Rhode Island derived the effect of this coupling on the natural frequency of the system by deriving a “resonance match condition.” Using the equation presented in their STTR report [10], and plugging in Equations 4, 5, 6, and 7, Equation (9) was derived.

$$\omega_{match} = \frac{\sqrt{(\omega_b + \omega_p)^2 + \frac{gm_p}{L_2M}} - \sqrt{(\omega_b - \omega_p)^2 + \frac{gm_p}{L_2M}}}{2} \quad (9)$$

Equation (9) solves for the angular frequency of the resulting system due to a coupled spring-mass system. In this equation, the second term within each radical,  $\frac{gm_p}{L_2M}$ , represents the inertial effect of the internal spring constant on the total mass of the buoy. In this term,  $g$  is gravity,  $m_p$  is the mass of the internal pendulum,  $M$  is the total mass of the buoy ( $m_b + \rho_w V m^* C_d$ ), and  $L_2$  is the length of the internal pendulum.  $\omega_b$  is the angular natural frequency of the buoy given by Equation 8.  $\omega_p$  is the angular frequency of the internal pendulum given by Equation (10).

$$\omega_{match} = \frac{\sqrt{(\omega_b + \omega_p)^2 + \frac{gm_p}{L_2M}} - \sqrt{(\omega_b - \omega_p)^2 + \frac{gm_p}{L_2M}}}{2} \quad (10)$$

Recognizing that  $m_p$  will always be a fraction of  $m_b$  when an internal pendulum load is carried within the buoy, we can utilize a ratio  $p^*$  defined as the mass of the internal pendulum load  $m_p$  relative to the mass of the buoy,  $m_b$ . Thus, for a fixed or non-moving pendulum load within a buoy,  $p^* = 0$ , whereas  $p^* = 0.8$  indicates that the free-swinging pendulum mass constitutes 80% of the buoy mass.

Essentially,  $p^* = m_p/m_b$ . Then replacing  $m_p$  with  $m_b p^*$  and  $m_b$  with  $\rho_w V m^*$ , Equation (9) can be reduced to

$$\omega_{match} = \frac{\sqrt{(\omega_b + \omega_p)^2 + \frac{gm_p}{L_2M}} - \sqrt{(\omega_b - \omega_p)^2 + \frac{gm_p}{L_2M}}}{2} \quad (11)$$

Equation (11) defines the resultant natural frequency of a buoyant tethered buoy with a free-swinging internal pendulum load in terms of  $p^*$ ,  $m^*$ ,  $Ca$  (typically 1 for cylinder),  $\omega_b$ , and  $\omega_p$ . Similar to Equation (8), this natural frequency is not affected by buoy diameter  $D$ , but is driven by the buoy and pendulum mass relative to displaced fluid mass ( $m^*$  and  $p^*$ , respectively) and length of the internal pendulum,  $L_2$ .

Figure 8 plots this  $\omega_{match}$  as a function of  $m^*$  and family of curves representing a range of  $p^*$  values. For a 0.25-meter-diameter x 0.60-meter-long buoy in 0.25 meters/second flow, a vortex shedding frequency,  $f_{vs}$  of 0.20 cycles/second is calculated using the Strouhal number relationship in Equation (1). To have any chance of matching this excitation frequency, buoy and pendulum masses must be adjusted against displaced fluid mass. For example:

$m^* = 0.65$  for a fixed pendulum load ( $p^* = 0$ ), or  $m^* = 0.40$  for a pendulum mass ratio  $p^*$  of 0.1.

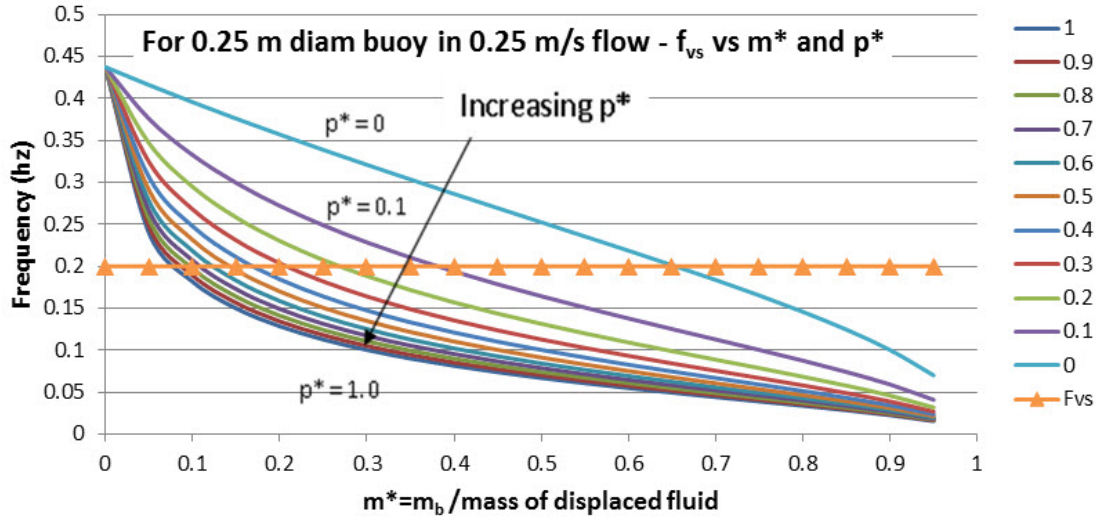


Figure 8. Natural frequency for range of  $m^*$  ( $m_b$  /mass of displaced fluid) and  $p^*$  (pendulum mass/buoy mass) ratios are modeled. Excitation frequency  $f_{vs}$  is fixed (horizontal line) for given buoy diameter and flow velocity;  $f_{vs}$  matches natural buoy frequencies at line intersections.

This model currently excludes any effects of damping. As conventional physics describes, the natural frequency of a pendulum will be shifted by a damping effect. This shift is described by Equation (12). In this equation,  $\omega_{peak}$  is the new shifted natural frequency of the system,  $\omega_{match}$  is the non-damped natural frequency of the buoy with an internal pendulum mass, and  $\zeta$  is the damping coefficient. For the internal pendulum, this will be an appropriate assumption until the electrical and mechanical damping from the generator is introduced to the system. For the buoy natural frequency, this assumption should hold true as the predicted velocities of the buoy's oscillation are fairly small. The damping coefficient will be determined experimentally later at SSC Pacific.

$$\omega_{peak} = \sqrt{1 - \zeta^2} \omega_{match} \quad (12)$$



## 4. CONCLUSIONS

A derivation of a non-dimensionalized math model was presented for predicting oscillation frequencies of a submerged tethered buoy. The model included a prediction of the buoy excitation frequencies due to vortex shedding. To match this excitation frequency with buoy natural frequencies, this model included coupling effects of an internal pendulum and added mass of the buoy, but excluded viscous damping. This model did not include coupling of the buoy motion on the vortex shedding frequencies.

This report also presented a linear generator system that could be used internally in an upright buoy to produce power. Simple power tests were conducted using machine and manual actuation of the magnets.

Future work on this project will include (1) laboratory and field testing to validate the VIV oscillation model, (2) a possible adjustment of the model to include a coupling effect of buoy motion with vortex shedding as well as viscous damping, and (3) incorporation of a generator into a buoy design to validate power output predictions. The effects of the generator on the model will then be included.



## 5. REFERENCES

1. VIVACE, [www.vortexhydroenergy.com/developments/](http://www.vortexhydroenergy.com/developments/), accessed 30 July 2013.
2. Wind Belt. 2013. [www.popularmechanics.com/science/energy/solar-wind/4224763](http://www.popularmechanics.com/science/energy/solar-wind/4224763), accessed 30 July 2013.
3. A. Phipps, D. Phung, M. Kerber, B. Dick, A. Powers, and R. Waters, “Development of Kinetic Energy Harvesting Systems for Vehicle Applications,” <http://ieeexplore.ieee.org/stamp/stamp.jsp?arnumber=06127010>.
4. M. R. Gharib. 1999. “Vortex Induced Vibration, Absence of Lock-in, and Fluid Force Deduction.” Thesis. California Institute of Technology. [http://thesis.library.caltech.edu/2874/1/Gharib\\_mr\\_1999.pdf](http://thesis.library.caltech.edu/2874/1/Gharib_mr_1999.pdf), accessed 6 June 2013.
5. R. D. Blevins. 1990. *Flow-induced Vibration*. 2nd ed. Van Nostrand Reinhold, New York, NY.
6. C. H. Colwell. “PhysicsLAB.” *PhysicsLAB*. N.p., n.d. Web. 10 June 2013.
7. H. O. Berteaux. 1991. *Coastal and Oceanic Buoy Engineering*. Woods Hole Oceanographic Institution, Woods Hole, MA.
8. A. Khalak and C.H.K. Williamson. 1999. “Motions, Forces, and Mode Transitions in Vortex-Induced Vibrations at Low Mass-damping,” *Journal of Fluids and Structures* 13:813–851.
9. R. D. Blevins and C. S. Coughran. 2009 (30 September). “Experimental Investigation of Vortex-Induced Vibration in One and Two Dimensions with Variable Mass, Damping, and Reynolds Number,” *Journal of Fluids Engineering* 131(10):101–202.
10. Electro Standards Laboratories. 2009 (20 February), “Ocean Energy Extraction for Sensor Applications.”, STTR Phase I Final Technical Report, Contract N00014-08-M-0277. Cranston, RI.



**REPORT DOCUMENTATION PAGE**

*Form Approved  
OMB No. 0704-01-0188*

The public reporting burden for this collection of information is estimated to average 1 hour per response, including the time for reviewing instructions, searching existing data sources, gathering and maintaining the data needed, and completing and reviewing the collection of information. Send comments regarding this burden estimate or any other aspect of this collection of information, including suggestions for reducing the burden to Department of Defense, Washington Headquarters Services Directorate for Information Operations and Reports (0704-0188), 1215 Jefferson Davis Highway, Suite 1204, Arlington VA 22202-4302. Respondents should be aware that notwithstanding any other provision of law, no person shall be subject to any penalty for failing to comply with a collection of information if it does not display a currently valid OMB control number.

**PLEASE DO NOT RETURN YOUR FORM TO THE ABOVE ADDRESS.**

<b>1. REPORT DATE (DD-MM-YYYY)</b> September 2014		<b>2. REPORT TYPE</b> Final		<b>3. DATES COVERED (From - To)</b>	
<b>4. TITLE AND SUBTITLE</b>  Output from Linear Generator for VIV-driven Buoys				<b>5a. CONTRACT NUMBER</b>	
				<b>5b. GRANT NUMBER</b>	
				<b>5c. PROGRAM ELEMENT NUMBER</b>	
<b>6. AUTHORS</b>  Wayne Liu                      Brian D'Angelo Jack Dea                        ASEE Kyle Wendler Brian Dick <b>SSC Pacific</b>				<b>5d. PROJECT NUMBER</b>	
				<b>5e. TASK NUMBER</b>	
				<b>5f. WORK UNIT NUMBER</b>	
<b>7. PERFORMING ORGANIZATION NAME(S) AND ADDRESS(ES)</b>  SSC Pacific, 53560 Hull Street, San Diego, CA 92152-5001				<b>8. PERFORMING ORGANIZATION REPORT NUMBER</b>  TR 2048	
<b>9. SPONSORING/MONITORING AGENCY NAME(S) AND ADDRESS(ES)</b>  In-house Laboratory Independent Research Program SSC Pacific, 53560 Hull Street, San Diego, CA 92152-5001				<b>10. SPONSOR/MONITOR'S ACRONYM(S)</b>	
				<b>11. SPONSOR/MONITOR'S REPORT NUMBER(S)</b>	
<b>12. DISTRIBUTION/AVAILABILITY STATEMENT</b> Approved for public release.					
<b>13. SUPPLEMENTARY NOTES</b> This is work of the United States Government and therefore is not copyrighted. This work may be copied and disseminated without restriction.					
<b>14. ABSTRACT</b>  A derivation of a non-dimensionalized math model was presented for predicting oscillation frequencies of a submerged tethered buoy. The model included a prediction of the buoy excitation frequencies due to vortex shedding. To match this excitation frequency with buoy natural frequencies, this model included coupling effects of an internal pendulum and added mass of the buoy, but excluded viscous damping. This model did not include coupling of the buoy motion on the vortex shedding frequencies.  This report also presents a linear generator system that could be used internally in an upright buoy to produce power. Simple power tests were conducted using machine and manual actuation of the magnets.  Future work on this project will include (1) laboratory and field testing to validate the VIV oscillation model, (2) a possible adjustment of the model to include a coupling effect of buoy motion with vortex shedding as well as viscous damping, and (3) incorporation of a generator into a buoy design to validate power output predictions. The effects of the generator on the model will then be included					
<b>15. SUBJECT TERMS</b> Mission Area: Maritime Systems linear generator                      buoy oscillation                      energy harvesting buoy excitation modeling              vortex induced vibrations              power voltage					
<b>16. SECURITY CLASSIFICATION OF:</b>			<b>17. LIMITATION OF ABSTRACT</b>	<b>18. NUMBER OF PAGES</b>	<b>19a. NAME OF RESPONSIBLE PERSON</b>
<b>a. REPORT</b>	<b>b. ABSTRACT</b>	<b>c. THIS PAGE</b>			Wayne Liu
U	U	U	U	30	<b>19b. TELEPHONE NUMBER (Include area code)</b> (619) 553-1900



## INITIAL DISTRIBUTION

84300	Library	(2)
85300	Archive/Stock	(1)
55210	K. Wendler	(1)
55250	B. Dick	(1)
56480	W. Liu	(4)
56480	J. Y. Dea	(1)
Defense Technical Information Center		
Fort Belvoir, VA 22060-6218		(1)





Approved for public release.



SSC Pacific  
San Diego, CA 92152-5001